

# First Experimental Demonstration of Beam Storage by Three-Dimensional Spiral Injection Scheme for Ultra-Compact Storage Rings

R. Matsushita,<sup>1,\*</sup> H. Iinuma,<sup>2,†</sup> S. Ohsawa,<sup>3</sup> H. Nakayama,<sup>3</sup>  
K. Furukawa,<sup>3</sup> S. Ogawa,<sup>3</sup> N. Saito,<sup>1,3</sup> T. Mibe,<sup>1,3</sup> and M. A. Rehman<sup>4,‡</sup>

<sup>1</sup>*Graduate School of Science, University of Tokyo, 7-3-1 Hongo, Bunkyo-ku, Tokyo 113-0033, Japan*

<sup>2</sup>*Graduate School of Science and Engineering, Ibaraki University, Mito, Ibaraki 310-8512, Japan*

<sup>3</sup>*High Energy Accelerator Research Organization, 1-1 Oho, Tsukuba, Ibaraki 305-0801, Japan*

<sup>4</sup>*The Graduate University for Advanced Studies, Kanagawa 240-0193, Japan*

Three-dimensional spiral injection scheme enables storage in ultra-compact rings with nanosecond revolution period. We report the first successful storage of a 297 keV/c electron beam in a 22 cm weak-focusing storage ring with a 4.7 ns revolution period using multi-turn vertical kick with a 140 ns kicker pulse. Using a scintillating-fiber detector, we observe a signal exceeding  $5\sigma$  of the pre-injection rms noise for  $\geq 1\ \mu\text{s}$ , confirming beam storage. By varying the weak-focusing field configuration and measuring the stored beam distribution, we show that the storage beam resides within the predicted region by Monte Carlo simulations. This result is a key proof-of-principle for realizing ultra-compact storage rings for next-generation precision measurements including the muon experiments at J-PARC and PSI.

*Introduction*— Storage rings have played a central role in accelerator science since their first realization as colliders in the 1960s [1–3]. Their applications now span a wide range of fields, including particle and nuclear physics, synchrotron light sources, medical treatments, and various industrial applications. As these applications have expanded, injection methods have undergone continuous development. Conventional transverse injection relies on a pulsed kicker magnet that produces a localized dipole field which steers the injected beam toward the stored orbit. This traditional two-dimensional approach has matured over several decades and evolved into the well-established local bump orbit technique [4]. Ongoing research has also generated next-generation concepts such as nonlinear or multipole kicker injection [5, 6], swap-out injection [7], and longitudinal injection [8]. These developments have largely been motivated by advanced light-source facilities where ultralow emittance of storage beam requires extremely precise control and injection into very narrow dynamic apertures [9].

The present study addresses a different direction of progress. We focus on the ultra-compact storage rings, since a smaller ring reduces the region in which the experimental environment must be controlled for physics measurements, for example with respect to magnetic field uniformity and the installation of large-scale detector components. These features are especially important for next-generation precision-measurement experiments.

However, ultra-compact storage rings face a fundamental difficulty. As the size of the ring becomes smaller, the

revolution period of the circulating beam decreases to a few nanoseconds. Under these conditions, conventional injection schemes become challenging because they require strong pulsed magnetic fields with nanosecond-scale rise and fall times. Even state-of-the-art developments for the ILC damping ring demonstrated switching times of approximately 3 ns [10], and achieving significantly faster performance remains technically demanding. This limitation has formed a major obstacle in the realization of ultra-compact storage rings. For nanosecond revolution period, injection with minimal perturbation requires a kick confined to single turn, placing simultaneous demands on both switching speed and peak field that are difficult to meet with conventional pulsed-power systems.

A concept proposed in 2016 by *H. Iinuma et al.* [11] offers a solution. The idea is known as the *three-dimensional spiral injection scheme*, and it avoids the time-scale limitation by extending the injection orbit into the vertical direction. Instead of injecting the beam parallel to the solenoidal axis, the beam enters the solenoid-type storage magnet with a controlled pitch angle. This non-parallel injection causes the beam to experience the fringe field of the solenoid, which provides an initial vertical steering force. The storage region is defined by a weak-focusing magnetic potential [12, 13] located near the mid-plane of the magnet. As the injected beam toward this region, the sign of the fringe field changes due to the weak-focusing field and produces an upward vertical force. To counteract this effect, the spiral injection concept employs a pulsed kicker and this supplies a small vertical kick to reduces pitch angle during many consecutive turns.

The accumulated effect of these repeated vertical kicks guides the injected beam into the weak-focusing potential, allowing stable storage. Because the required deflection is distributed over multiple turns, the method avoids the need for the extremely fast pulsed-power performance

\* Contact author: matsur@post.kek.jp

† Contact author: hiromi.iinuma.spin@vc.ibaraki.ac.jp

‡ Present address: China Spallation Neutron Source Science Center, Dongguan 523803, China, Institute of High Energy Physics, Chinese Academy of Sciences, Beijing 100049, China

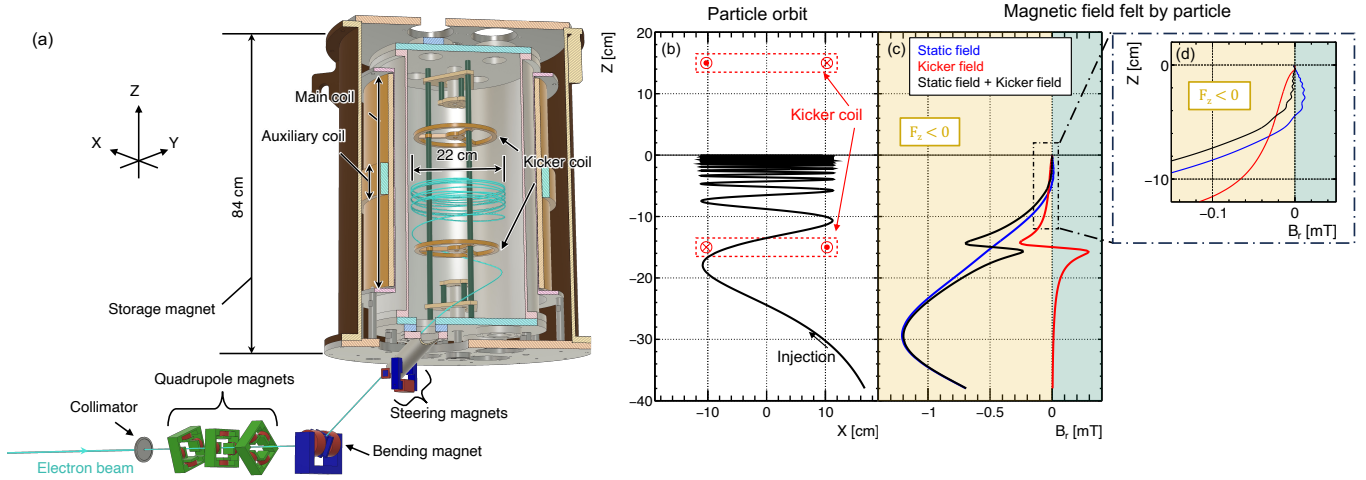


FIG. 1. (a): Overview of the demonstration beamline. The electron beam is generated by an electron gun and injected into the storage magnet through a transport line consisting of three rotatable quadrupole magnets, one bending magnet, and a pair of steering magnets. (b) X-Z projection of the reference particle orbit after injection. The storage midplane corresponds to  $Z = 0$  cm. (c),(d)  $B_r$  components along the reference particle orbit. Blue line shows the static magnetic field by the storage magnet. Red line shows the time-varying magnetic field by the kicker. The  $B_r < 0$  field during injection provides the downward steering to electrons required for beam storage in weak-focusing region.

that limits conventional two-dimensional injection.

The ability to implement this scheme paves the way toward ultra-compact storage rings that are impractical with conventional injection schemes. The ultra-compact rings are essential for precision measurements involving short-lived particles. The muon  $g - 2$ /EDM experiment at J-PARC [14] and the muEDM experiment at PSI [15] require the storage of relativistic beams in regions only a few tens of centimeters across, with revolution periods of only a few nanoseconds. Compact rings enable relativistic beams to be stored in a small, well-controlled volume, which is advantageous for precision measurements of short-lived particles. Beyond muon physics, ultra-compact weak-focusing rings could support high-precision mass spectrometry and electric-dipole-moment searches using various particle species.

No experimental demonstration had been reported until now. In this Letter we present the first successful storage of an electron beam using this method.

*Experimental setup*— A beamline was constructed [16] for the demonstration of the three-dimensional spiral injection scheme. Fig. 1(a) shows an overview of the demonstration beamline. An electron beam with momentum is  $p = 297 \text{ keV}/c$ , kinetic energy is  $E_{\text{kin}} = 80 \text{ keV}$  and pulsed width is 100 ns is generated using a thermionic electron gun [17] and a chopper system [18]. The transport line allows us to control the beam phase space and the injection orbit at the injection point. This transport line consists of three quadrupole magnets, one bending magnet, and a pair of steering magnets [16], then injected into the storage magnet with a 0.7 rad pitch angle, defined with respect to the horizontal (X-Y) plane.

The storage magnet consists of two solenoidal coils [19], main coil and auxiliary coil shown in Fig. 1(a), allow us to apply both solenoidal field and weak-focusing field in the beam storage region. By setting the coil currents  $I_{\text{MAIN}}$  and  $I_{\text{AUX}}$  with opposite polarities, we adjust the weak-focusing field potential (field index  $n \sim 10^{-2}$  in the storage region) while keeping the solenoidal field constant at  $B_z = 8.77 \text{ mT}$  on the storage plane ( $Z = 0$  cm). Fig. 1(b) shows the projected reference particle orbit in the X-Z plane and Fig. 1(c) and (d) show the corresponding  $B_r$  component along the reference orbit. After injection, the beam follows a spiral orbit thanks to the  $B_z$  component and simultaneously being steered downward ( $Z < 0$ ) thanks to the fringe field of  $B_r < 0$ . Inside the weak-focusing region, the  $B_r > 0$  from static weak-focusing field applies an upward force. To counter this, a 45 A, 140 ns pulsed current is applied to the kicker coils, inductance  $L = 1.3 \mu\text{H}$ , at  $Z = \pm 15 \text{ cm}$ , generating a  $B_r < 0$  field that maintains the downward steering and enables beam storage.

A detector using plastic-scintillating-fiber (SciFi), *SciFi-probe* [20], which can be inserted into the storage region, is utilized to measure the storage beams. The SciFi-probe consists of a 1 mm-diameter and 20 cm-long SciFi, which is long enough to cover the entire storage region vertically. The scintillation signal is read out with a photomultiplier tube (PMT). Because the CSDA range of a  $p = 297 \text{ keV}/c$  electron in the SciFi is about  $100 \mu\text{m}$  [21], the measurement is destructive.

In a measurement, the SciFi-probe is inserted vertically from above with its tip positioned at an insertion depth  $Z$ , which is measured from the storage midplane

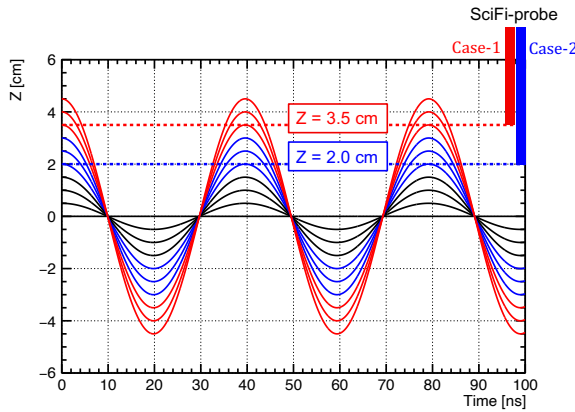


FIG. 2. Principle of SciFi-probe measurement. Solid lines show the stored particle trajectories with vertical betatron oscillation. Stored particles with vertical betatron amplitude greater than  $Z$  [cm], which is the tip position of the SciFi-probe, generate signals. Case-1, SciFi-probe is inserted up to  $Z = 3.5$  cm, measures particles with vertical amplitude  $\geq 3.5$  cm shown by red lines. Similarly, Case-2, SciFi-probe is inserted up to  $Z = 2.0$  cm, measures those with amplitude  $\geq 2.0$  cm shown by red and blue lines.

( $Z = 0$  cm), and particle hits generate a signal. Because stored particles perform vertical betatron oscillations, the integrated signal at a given  $Z$  is proportional to the population whose vertical amplitude exceeds that depth (Fig. 2). Since the stored particles also perform betatron oscillations in the radial direction simultaneously with vertical betatron oscillations, the SciFi-probe does not measure all stored particles within a single vertical betatron oscillation period. We thus integrate the SciFi-probe signal over a sufficiently long time window to cover a wide range of betatron phases. In this Letter, we define beam storage operationally as observing a SciFi-probe signal that exceeds  $5\sigma_{\text{noise}}$  for  $1\mu\text{s}$  or longer, which is ten times longer than the injected pulse width of  $100\text{ ns}$  and corresponds to more than  $200$  revolutions, where  $\sigma_{\text{noise}}$  is the standard deviation (rms fluctuation) of the voltage in a pre-injection time window. This conservative criterion is introduced to distinguish true storage from non-stored or transiently circulating particles that may survive for only a few turns before escaping the weak-focusing region.

A plastic scintillator is installed on the bottom surface of the storage chamber as a beam loss monitor to observe time structure of reflected beams that are not captured in the storage region during injection. Information from this beam loss monitor is used for tuning beam injection trajectory.

*Experimental results*— Beam storage was confirmed using the operational criterion defined above based on the SciFi-probe waveform. Fig. 3 shows the waveforms from the SciFi-probe, the beam-loss monitor and kicker

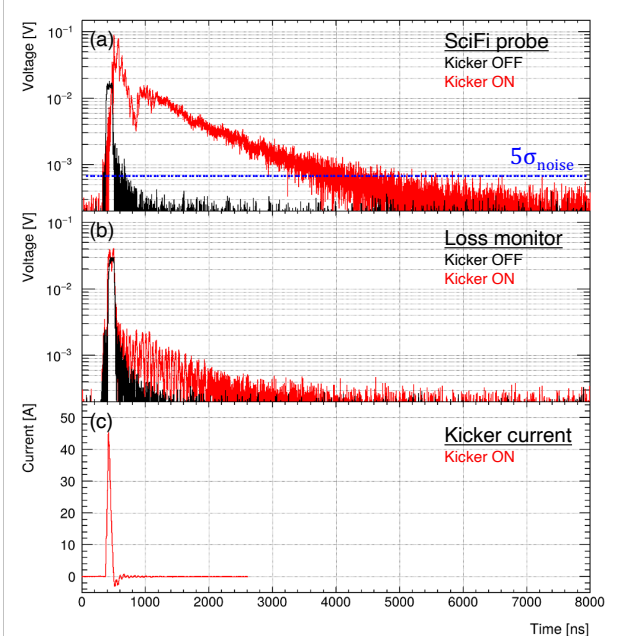


FIG. 3. Example of measured signals. (a): SciFi-probe signal measured within the weak-focusing region. Blue line shows the threshold of  $5\sigma_{\text{noise}}$ . (b): Loss-monitor signal downstream of the storage region. (c): Kicker current waveform measured using a Rogowsky coil. Red and black lines correspond to the with and without kicker conditions, respectively. In this example, the SciFi-probe is inserted up to the storage midplane and SciFi covered the range from  $Z = 0$  cm to  $Z = 20$  cm. Each waveform is an average over 1000 shots.

current for cases with and without the kicker. With the kicker activated, the SciFi-probe signal remains above  $5\sigma_{\text{noise}}$  for longer than  $1\mu\text{s}$ , thereby satisfying our definition of beam storage and indicating successful beam storage in the weak-focusing region. The beam-loss monitor simultaneously detected a signal induced by reflected beams, at the expected timing relative to the kicker pulse. In contrast, without the kicker the SciFi-probe signal has a duration of order  $100\text{ ns}$  comparable to the injected pulse width and does not satisfy the  $5\sigma_{\text{noise}}$  for  $1\mu\text{s}$  storage criterion, indicating that the beam is not stored under these conditions. This clear contrast demonstrates that three-dimensional spiral injection enables beam storage in ultra-compact storage rings.

During the first several hundred nanoseconds after injection, the stored particles perform coherent vertical betatron oscillations. This coherence produced a periodic modulation in the SciFi waveform. Although the modulation originates from the vertical betatron motion, its period does not correspond to the betatron oscillation period itself. The difference arises because the injected beam has a pulse width that is longer than one betatron period, so the SciFi-probe samples particles with a wide distribution of betatron phases within each injection pulse. As time evolves, the periodic structure grad-

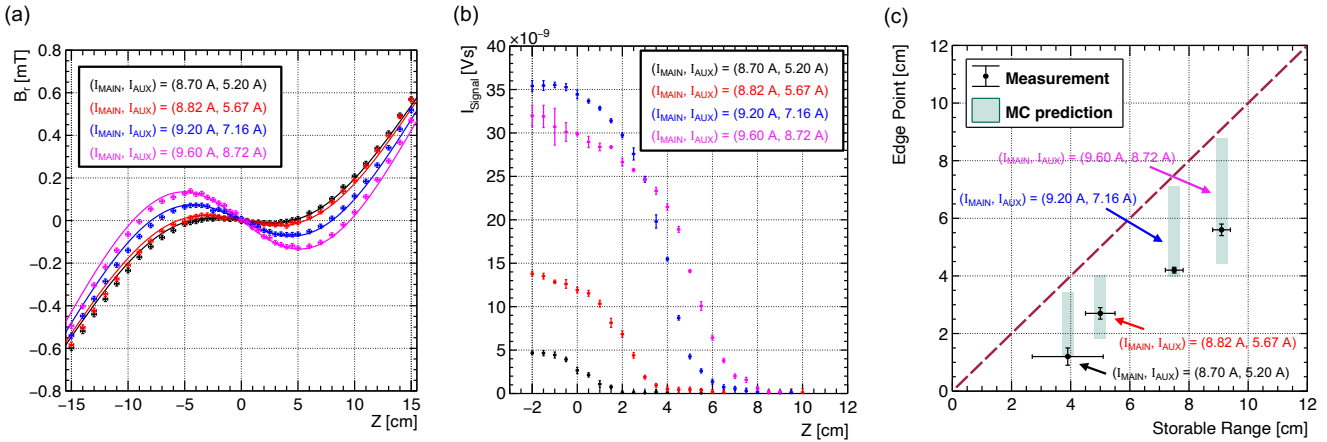


FIG. 4. Weak-focusing field dependence of the stored beam distribution. (a): Weak-focusing field configurations. Colored points denote measurement result, and colored lines denote finite element calculations performed with Opera [22]. (b): Z-scan results under the four field configurations. The vertical axis shows the time-integrated SciFi-probe signal,  $I_{\text{Signal}} = \int V_{\text{Signal}}(t) dt$ , where  $V_{\text{Signal}}(t)$  is the measured voltage as a function of time. The integral is evaluated over the time window from  $t = 560$  ns to 9000 ns, starting just after the end of the kicker pulse. (c): Comparison of measured stored beam ranges with Monte Carlo predictions. Blue shaded regions show the expected region of MC simulation. Black points show the measurement result from field measurement and Z-scan measurement.

ually decreases in visibility. This reduction is caused by the position dependence of the weak-focusing magnetic field, which introduces small variations in the betatron frequency and leads to phase mixing among the stored particles.

The overall measured storage signal exceeded  $1\ \mu\text{s}$ , shown in Fig. 3(a). This signal duration is more than one order of magnitude longer than the loss time observed without the kicker and provides a quantitative demonstration that multi-turn vertical steering enables stable particle storage even when the revolution period is as short as five nanoseconds. The observed signal duration is dominated by scattering within the SciFi probe, which is inserted into the storage region for measurement. The intrinsic storage lifetime of the beam is therefore expected to be significantly longer.

We confirmed that the accumulated beam is stored by the weak-focusing field through a series of Z-scan measurements performed under four different field configurations. The magnetic-field distributions for these configurations are presented in Fig. 4(a). For each configuration, the SciFi probe was inserted to multiple vertical positions, and the time-integrated signal recorded at each position is shown in Fig. 4(b), which is Z-scan. Fig. 4(c) compares the measured upper boundary of the storage beam distribution, which is defined as the position where the integrated signal decreases to five percent of its maximum value, with Monte Carlo (MC) predictions of the storable range for each weak-focusing field configuration. The measurement results for each field configuration agree with MC predictions. This result verifies that the spatial distribution of the accumulated

beam is governed by the weak-focusing magnetic field and confirms that the observed beam storage originates from the intended magnetic field structure rather than accidental trapping or experimental artifacts. The dominant systematic uncertainty arises from the injection trajectory uncertainty, which has been evaluated and included in the MC predictions.

The present storage efficiency, defined as the fraction of electrons stored from one injected bunch, is well below 1% under the current injection conditions based on Monte Carlo simulations. The storage efficiency can be improved by XY-coupled transverse phase-space matching and a shorter injected bunch length achievable through upstream RF beam manipulation.

*Conclusions*— We have achieved the first experimental demonstration of beam storage by the three-dimensional spiral injection scheme. This demonstration establishes the technical feasibility of this scheme and provides a viable pathway toward ultra-compact storage rings required for next-generation precision experiments. The technique is a key enabling technique for the planned muon  $g - 2$ /EDM experiment at J-PARC and the muEDM experiment at PSI, and may open a new frontier in precision studies of short-lived particles.

*Acknowledgments*— We thank H. Hisamatsu, H. Someya, T. Suwada, Y. Okayasu, and Y. Yano for providing equipment used in this work, and K. Sasaki for help with magnetic field measurements. We also thank A. Tokuchi (Pulsed Power Japan Laboratory Ltd.) for manufacturing the pulsed-power supply for the kicker system and T. Ushiku (Next Create Service Ltd.) for manufacturing the magnets. We acknowledge general

support from the KEK Accelerator Injector LINAC group, technical support from the KEK Mechanical Engineering Center, and assistance with installation work from Futaba Kogyo Co., Ltd. This work was supported by JSPS KAKENHI Grants No. 26287055, No. 19H00673, No. 22K14061, and No. 23KJ0590.

---

[1] C. Bernardini, G. F. Corazza, G. Di Giugno, J. Haissinski, P. Marin, R. Querzoli, and B. Touschek, *Il Nuovo Cimento (1955-1965)* **34**, 1473 (1964).

[2] G. I. Budker, N. A. Kushnirenko, A. A. Naumov, A. P. Onuchin, S. G. Popov, V. A. Sidorov, A. N. Skrinskii, and G. M. Tumaikin, *Soviet Atomic Energy* **19**, 1467 (1965).

[3] G. K. O'Neill, in *2nd International Conference on High-Energy Accelerators* (1959) pp. 23–25.

[4] S. Y. Lee, *Accelerator Physics (Fourth Edition)* (World Scientific Publishing Company, 2018) pp. 86–87.

[5] K. Harada, Y. Kobayashi, T. Miyajima, and S. Nagahashi, *Phys. Rev. ST Accel. Beams* **10**, 123501 (2007).

[6] H. Takaki, N. Nakamura, Y. Kobayashi, K. Harada, T. Miyajima, A. Ueda, S. Nagahashi, M. Shimada, T. Obina, and T. Honda, *Phys. Rev. ST Accel. Beams* **13**, 020705 (2010).

[7] S. Henderson, in *Proc. 6th International Particle Accelerator Conference (IPAC'15), Richmond, VA, USA, May 3-8, 2015*, International Particle Accelerator Conference No. 6 (JACoW, Geneva, Switzerland, 2015) pp. 1791–1793.

[8] M. Aiba, M. Böge, F. Marcellini, A. Saá Hernández, and A. Streun, *Phys. Rev. ST Accel. Beams* **18**, 020701 (2015).

[9] M. Aiba, in *9th International Particle Accelerator Conference* (2018).

[10] T. Naito, H. Hayano, M. Kuriki, N. Terunuma, and J. Urakawa, *Nuclear Instruments and Methods in Physics Research Section A: Accelerators, Spectrometers, Detectors and Associated Equipment* **571**, 599 (2007).

[11] H. Iinuma, H. Nakayama, K. Oide, K. ichi Sasaki, N. Saito, T. Mibe, and M. Abe, *Nuclear Instruments and Methods in Physics Research Section A: Accelerators, Spectrometers, Detectors and Associated Equipment* **832**, 51 (2016).

[12] R. R. Wilson, *Phys. Rev.* **53**, 408 (1938).

[13] D. W. Kerst, *Phys. Rev.* **58**, 841 (1940).

[14] M. Abe *et al.*, *PTEP* **2019**, 053C02 (2019), arXiv:1901.03047 [physics.ins-det].

[15] T. Hu, *Nuclear and Particle Physics Proceedings* **346**, 40 (2024).

[16] M. A. Rehman, *A Validation Study on the Novel Three-Dimensional Spiral Injection Scheme with the Electron Beam for Muon g-2/EDM Experiment*, Ph.D. thesis, SO-KENDAI (2020), ph.D. thesis, <http://id.nii.ac.jp/1013/00006023/>.

[17] T. Sugimura, S. Ohsawa, and M. Ikeda, *Journal of Synchrotron Radiation* **15**, 258 (2008).

[18] R. Matsushita, M. Abe, H. Hirayama, K. Furukawa, H. Iinuma, T. Mibe, H. Nakayama, K. Oda, S. Ohsawa, M. Rehman, N. Saito, K. Sasaki, Y. Sato, M. Sugita, and T. Takayanagi, in *Proc. IPAC'21, International Particle Accelerator Conference No. 12* (JACoW Publishing, Geneva, Switzerland, 2021) pp. 809–812.

[19] M. A. Rehman, H. Iinuma, S. Ohsawa, H. Nakayama, H. Hisamatsu, K. Furukawa, and T. Mibe, in *Proc. 29th Linear Accelerator Conference (LINAC'18), Beijing, China, 16-21 September 2018* (2018) pp. 717–720.

[20] R. Matsushita, H. Iinuma, K. Oda, S. Ohsawa, H. Nakayama, M. A. Rehman, K. Furukawa, N. Saito, T. Mibe, and S. Ogawa, *Journal of Physics: Conference Series* **2687**, 022035 (2024).

[21] The electron CSDA range is obtained from the NIST ESTAR database [23], assuming polystyrene (PS) as a material for the scintillating fiber.

[22] Dassault Systèmes, Opera-3d (simulia), <https://www.3ds.com/products/simulia/opera> (2026), accessed: 2026-02-03.

[23] M. J. Berger, J. S. Coursey, M. A. Zucker, and J. Chang, Estar, pstar, and astar: Computer programs for calculating stopping-power and range tables for electrons, protons, and helium ions (version 1.2.3), National Institute of Standards and Technology, Gaithersburg, MD (2005), online database, accessed 2026-01-06.